Research Article

Cui Chaopeng*, Zhu Xiangwei, Li Qiang, Zhang Min, and Zhu Guangping

Study on the erosion of Mo/ZrO_2 alloys in glass melting process

https://doi.org/10.1515/htmp-2020-0061
received November 01, 2019; accepted May 19, 2020

Abstract: The Mo/ZrO_2 electrode was prepared by combining hydrothermal synthesis with powder metallurgy, and this new electrode material has a totally different microstructure from the conventional electrode. The grain size of the new electrode was fine, and the size of ZrO_2 in the alloy reached 200 nm. According to the results, the $Mo–ZrO_2$ electrode has better performance, because the erosion occurs along the grain boundaries. Meanwhile, the new electrode, based on its fine grain, can effectively improve the corrosion resistance of the electrode.

Keywords: erosion, Mo/ZrO_2, electrode, grain size, grain boundaries, glass

1 Introduction

By virtue of its excellent performance such as high melting point, good thermal conductivity, low coefficient of expansion, excellent temperature strength, and superior corrosion resistance of glass, molybdenum alloys have been widely applied in the fields of melting optical glass, glass fiber, and high-grade refractory wool as an electrode material [1–6]. The corrosion resistance of the electrodes has become widely noted since the corrosion of the glass liquid can generate the surface grain of the molybdenum electrode. However, the grain size and the use performance of the molybdenum electrode can be improved by adding trace rare earth elements. In this paper, the quality and performance of the molybdenum electrodes are studied [7–10].

In the glass melting process, the properties of electrode material shall meet the requirements as below:

(1) good electrical conductivity, less electrical energy consumption;
(2) excellent mechanical strength at 1,700°C or above;
(3) smaller temperature sensitivity;
(4) outstanding mechanical properties;
(5) superior corrosion resistance of glass and refractory materials above 1,700°C;
(6) no bubble in the contact process of the glass melting;
(7) unchanged performance of the electrode during the using process.

Molybdenum and its alloy are considered as the best electrode material in the glass manufacturing industry, so the electrodes made of them accordingly can completely meet the above conditions. At present, coating is commonly used to improve the corrosion resistance of the molybdenum electrodes, but it has the shortcomings of poor shock resistance, thermal stability, and thermal erosion resistance. As a regard method, ZrO_2/Mo electrode can effectively improve the performance of electrode [11–16]. In addition to proposing a new method for preparing the ZrO_2/Mo alloy, this paper also studied the difference between the alloy prepared by new method preparation and the solid–solid preparation through the experiment, analyzed the performance of alloy, and explored the influences of second phases on the microstructure.

2 Experiment procedures

The precursor was prepared by the hydrothermal synthesis of $(NH4)_2Mo_4O_{13}{\cdot}2H_2O$ and $Zr(NO_3)_4{\cdot}3H_2O$, and the reference sample was prepared by solid–solid processing. By means of sintering the alloy-pressed billet in the size of ∅20 × 60 mm, alloy sintered compact in size of ∅17 × 58 mm was made, and the final size is ∅8 × 12 mm.

The test on the performance of corrosion resistance was conducted in glass liquid at 1,200°C for 300 h, of

* **Corresponding author: Cui Chaopeng,** School of Physics and Electronic Information/Information College, Huaibei Normal University, Huaibei 235000, Anhui Province, China; Anhui Province Key Laboratory of Pollutant Sensitive Materials and Environmental Remediation, e-mail: ccp273206157@163.com
Zhu Xiangwei, Li Qiang, Zhang Min, Zhu Guangping: School of Physics and Electronic Information/Information College, Huaibei Normal University, Huaibei 235000, Anhui Province, China; Anhui Province Key Laboratory of Pollutant Sensitive Materials and Environmental Remediation

Table 1: Physical property of ZrO_2/Mo alloy

Number	Content (wt%)	Density (g/cm^3)	Microhardness (HV)
1	0	9.7600	168.51
2	0.1	9.6298	210.19
3	0.5	9.5998	220.86
4	1.0	9.5528	228.45
5	1.5	9.4998	236.46
4*	1.0	9.3258	170.34

which the glass used was from the LCD screen. The scanning electron microscope (SEM, VEGA-3 SBH), energy dispersive spectrometer, and transmission electron microscope (TEM-2100) were adopted to observe the microstructures of samples before and after tensile tests.

3 Results and discussions

In the experiment, sintered samples were tested as shown in Table 1. With an increase in adding amount, the porosity and hardness increased while the density of the alloy decreased. The chemical analysis indicated that the ZrO_2 content was the same as that in the table. With the increase of adding amount, the porosity and microhardness increased, while the density was decreased.

Sample 4* is the reference sample made by solid–solid processing, and its second phase is heavily concentrated. The microstructure prepared by different methods is shown in Figure 1. It can be seen that based on the new method, the alloys made are dispersed; the second phase is small and dispersed; and the second phase of 4* reference sample is bulky and concentrated. Another finding is that the grain of alloy prepared by the new method is finer. As can be observed from Figure 2, with the increase of adding amount, the grain of alloy is reduced, which will influence the performance of the electrode. Therefore, the alloy prepared through using the new method has better distribution and small grain size, and the second phase particle size is only 200 nanometers as shown in the figure [17–23].

After 300 h experiment in glass liquid, the grain size before and after the experiment was compared. As shown in Figure 2, the grain of alloy was decreased with the

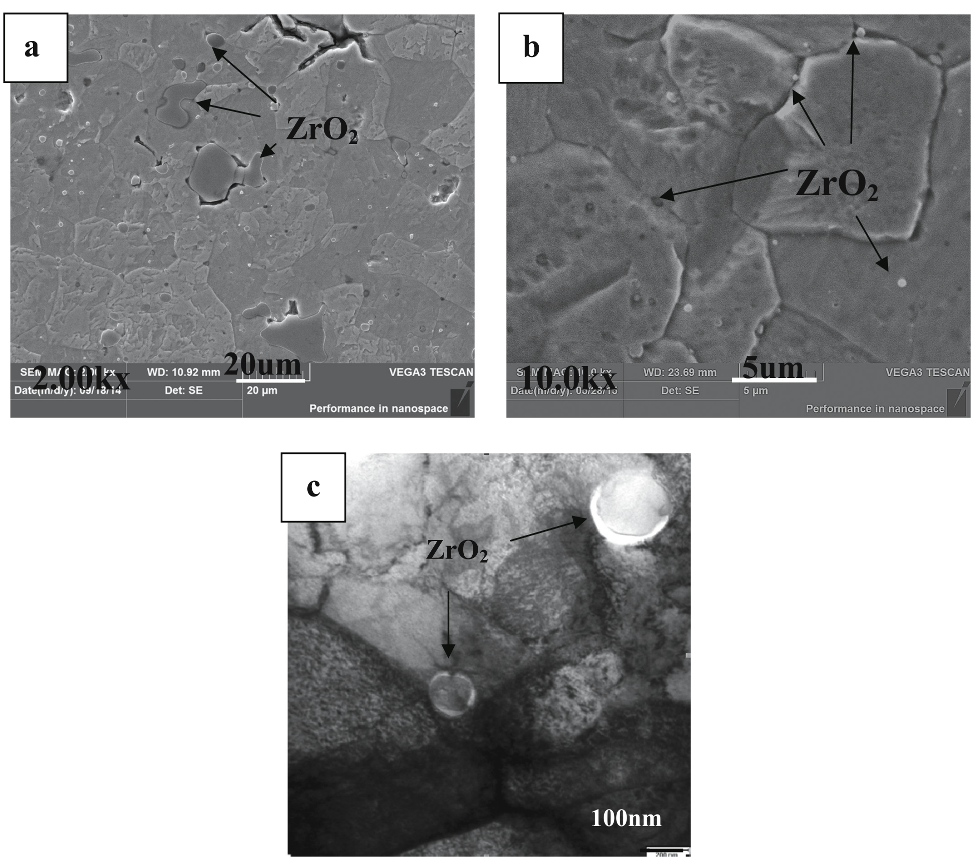

Figure 1: Photos of ZrO_2/Mo alloy: (a) 4* × 2.00k× (reference sample), (b) 5 × 10.00k× (new method), (c) TEM of alloy.

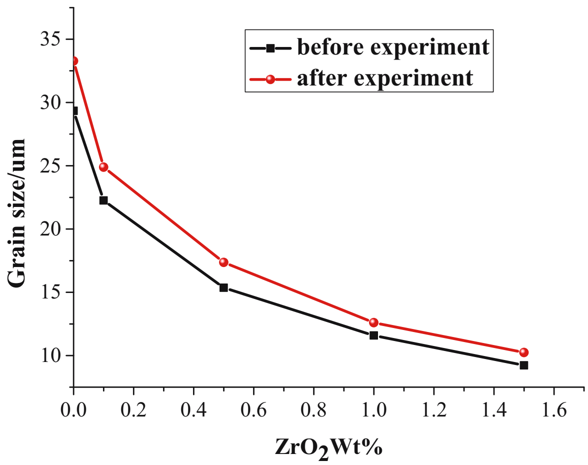

Figure 2: Grain size before and after the experiment.

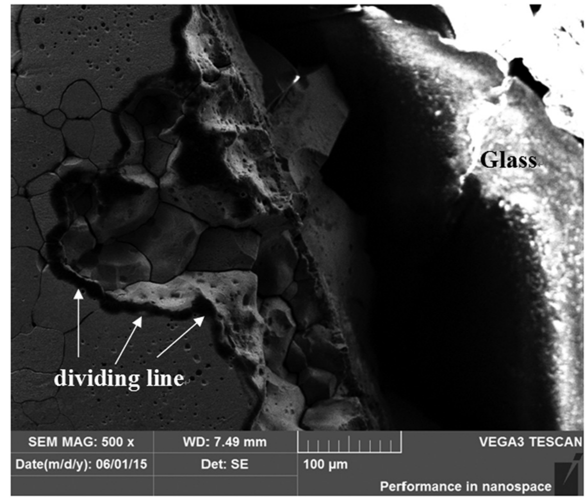

Figure 4: SEM photos after the experiment.

increase of adding amount, but its size grew slowly at the end of the experiment when reaching the temperature of 1,200°C. This will influence the corrosion resistance of the electrode in glass liquid.

The corrosion depth of the glass was observed and measured after the experiment. In Figure 3, with the addition of ZrO_2, the corrosion depth became shorter than pure molybdenum, of which sample 5 has the shortest corrosion depth. The surface and interior morphology of the samples indicate that the glass generates an obvious erosion effect on the surface of the samples. In Figure 4, the surface of the material underwent great changes, such as the obvious erosion interface on the surface of the sample, significantly larger grain outside the boundary and the presence of vugs in grains near the edge. In contrast, the organizational structure in the sample did not change significantly, except for the twice growth of grains. The organizational difference among the 5 samples is grain size. Figure 4 also displays that erosion occurred along the grain boundaries. After the heat treatment, the grains of the alloy and the chink of grains grew larger than before; the viscosity of glass was rapidly decreased, and the erosion of the brick was accelerated. Vugs are the cause of lower relative density; the microstructure of alloy was loosely organized; the vugs triggered the increase of contact area, which in turn led to a lower erosion resistance of the samples. With the increase of adding amount, the grains became finer and the microstructure became homogeneous so that the alloy with high content possesses a strong resistance to erosion.

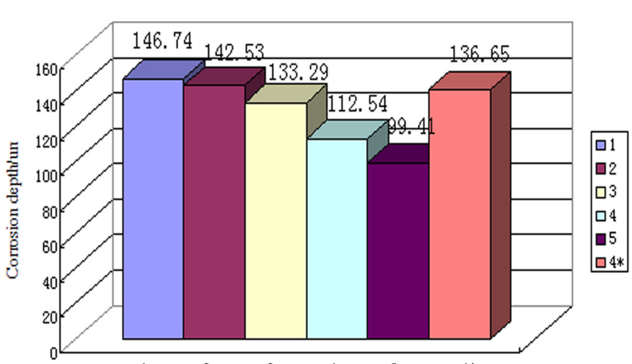

Figure 3: Corrosion depth of the glass.

Acknowledgments: This work was supported by the Anhui Natural Science Foundation (1908085QF293, 1908085QA36, KJ2019B14).

References

[1] Sharma, I. G., S. P. Chakraborty, and A. K. Suri. Preparation of TZM alloy by aluminothermic smelting and its characterization. *Journal of Alloys and Compounds*, Vol. 393, No. 1–2, 2005, pp. 122–127.

[2] Cockeram, B. V. The mechanical properties and fracture mechanisms of wrought low carbon arc cast (LCAC), molybdenum–0.5pct titanium–0.1pct zirconium (TZM), and oxide dispersion strengthened (ODS) molybdenum flat products. *Materials Science and Engineering A*, Vol. 418, No. 1–2, 2006, pp. 120–136.

[3] Iorio, L. E., B. P. Bewlay, and M. Larsen. Analysis of AKS- and lanthana-doped molybdenum wire. *International Journal of Refractory Metals and Hard Materials*, Vol. 24, No. 4, 2006, pp. 306–310.

[4] Mrotzek, T., A. Hoffmann, and U. Martin. Hardening mechanisms and recrystallization behaviour of several molybdenum alloys. *International Journal of Refractory Metals and Hard Materials*, Vol. 24, No. 4, 2006, pp. 298–305.

[5] Fan, J., M. Lu, H. Cheng, J. Tian, and B. Huang. Effect of alloying elements Ti, Zr on the property and microstructure of molybdenum. *International Journal of Refractory Metals and Hard Materials*, Vol. 27, No. 1, 2009, pp. 78–82.
[6] Liu, G., G. J. Zhang, F. Jiang, X. D. Ding, Y. J. Sun, J. Sun, et al. Nanostructured high-strength molybdenum alloys with unprecedented tensile ductility. *Nature Materials*, Vol. 12, No. 4, 2013, pp. 344–350.
[7] Cockeram, B. V. The role of stress state on the fracture toughness and toughening mechanisms of wrought molybdenum and molybdenum alloys. *Materials Science and Engineering A*, Vol. 528, No. 1, 2010, pp. 288–308.
[8] Gludovatz, B., S. Wurster, A. Hoffmann, and R. Pippan. Fracture toughness of polycrystalline tungsten alloys. *International Journal of Refractory Metals and Hard Materials*, Vol. 28, No. 6, 2010, pp. 674–678.
[9] Mrovec, M., C. Elsässer, and P. Gumbsch. Atomistic simulations of lattice defects in tungsten. *International Journal of Refractory Metals and Hard Materials*, Vol. 28, No. 6, 2010, pp. 698–702.
[10] Oertel, C. G., I. Hünsche, W. Skrotzki, A. Lorich, W. Knabl, J. Resch, et al. Influence of cross rolling and heat treatment on texture and forming properties of molybdenum sheets. *International Journal of Refractory Metals and Hard Materials*, Vol. 28, No. 6, 2010, pp. 722–727.
[11] Schade, P., and H. M. Ortner. 100 years of doped tungsten wire. *International Journal of Refractory Metals and Hard Materials*, Vol. 28, No. 6, 2010, pp. 648–660.
[12] Cui, C., Y. Gao, S. Wei, G. Zhang, Y. Zhou, K. Pan, et al. Preparation and properties of ZrO2/Mo alloys. *High Temperature Materials and Processes*, Vol. 36, No. 2, 2017, pp. 163–166.
[13] Cui, C., Y. Gao, S. Wei, G. Zhang, Y. Zhou, and X. Zhu. Microstructure and high temperature deformation behavior of the Mo-ZrO2 alloys. *Journal of Alloys and Compounds*, Vol. 716, 2017, pp. 321–329.
[14] Cui, C., Y. Gao, S. Wei, G. Zhang, G. Zhou, Y. Pan, et al. The Mechanical properties of the Mo-0.5Ti and Mo-0.1Zr alloys at room temperature and high temperature annealing. *High Temperature Materials and Processes*, Vol. 36, No. 2, 2017, pp. 167–173.
[15] Chaopeng, C., Z. Xiangwei, L. Shulong, and L. Qiang. Effect of nano-sized ZrO2 on the recrystallization of Mo alloy. *Journal of Alloys and Compounds*, Vol. 752, 2018, pp. 308–316.
[16] Cui, C., X. Zhu, S. Liu, Q. Li, M. Zhang, G. Zhu, et al. Effect of nano-sized ZrO2 on high temperature performance of Mo-ZrO2 alloy. *Journal of Alloys and Compounds*, Vol. 768, 2018, pp. 81–87.
[17] Zhou, G., Z. Ren, L. Wang, B. Sun, S. Duan, and Q. Song. Artificial and wearable albumen protein memristor arrays with integrated memory logic gate functionality. *Materials Horizons*, Vol. 6, No. 9, 2019, pp. 1877–1882.
[18] Zhou, G., Z. Ren, L. Wang, J. Wu, B. Sun, A. Zhou, et al. A facile gaseous sulfur treatment strategy for Li-rich and Ni-rich cathode materials with high cycling and rate performance. *Nano Energy*, Vol. 63, 2019, id. 103887.
[19] Zhou, G., Z. Ren, B. Sun, J. Wu, Z. Zou, S. Zheng, et al. Capacitive effect: an original of the resistive switching memory. *Nano Energy*, Vol. 68, 2020, id. 104386.
[20] Sun, B., P. Han, W. Zhao, Y. Liu, and P. Chen. White-light-controlled magnetic and ferroelectric properties in multiferroic BiFeO3 square nanosheets. *The Journal of Physical Chemistry C*, Vol. 118, No. 32, 2014, pp. 18814–18819.
[21] Sun, B., H. Li, L. Wei, and P. Chen. Hydrothermal synthesis and resistive switching behaviour of WO3/CoWO4 core–shell nanowires. *CrystEngComm*, Vol. 16, No. 42, 2014, pp. 9891–9895.
[22] Zhou, Y., Y. Gao, S. Wei, and Y. Hu. Characterization of Al_2O_3 in high-strength Mo alloy sheets by high-resolution transmission electron microscopy. *Microscopy and Microanalysis*, Vol. 22, No. 1, 2016, pp. 122–130.
[23] Cui, C., Y. Gao, S. Wei, G. Zhang, Y. Zhou, X. Zhu, et al. Study on preparation and properties of molybdenum alloys reinforced by nano-sized ZrO_2 particles. *Applied Physics A*, Vol. 122, No. 3, 2016, id. 214.